Nanoscale

PAPER

View Article Online
View Journal | View Issue

Cite this: *Nanoscale*, 2026, **18**, 5805

Aqueous dispersion of carbon nanotubes by chlorine dioxide oxidation

Yuki Itabashi, [a] Ai Sunami,[a] Kaoru Maeno,[a] Hiroshi Ueno, [b,c] Takashi Itoh,[b] Hiroshi Fukumura [c,d] and Kei Ohkubo *[a,e]

The poor solubility and dispersibility of single-walled carbon nanotubes (SWCNTs) in aqueous media remain critical limitations for their practical application because conventional oxidative treatments typically require harsh conditions that degrade the nanotube structure. Here, we report a simple and scalable method for dispersing SWCNTs in water *via* chlorine dioxide ($ClO_2^{\bullet}$)-mediated oxidation under ambient conditions. The treatment selectively introduced oxygenated functionalities—including hydroxy, carbonyl, and carboxy groups—onto the CNT surface while preserving the tubular framework, as confirmed by transmission electron microscopy, Raman spectroscopy, and X-ray photoelectron spectroscopy analyses. The resulting dispersions exhibited long-term colloidal stability without the need for surfactants, supported by a strongly negative ζ potential (–41.6 mV). Importantly, electronic conductivity was largely maintained: the resistivity of oxidized CNT films was only threefold higher than that of sodium cholate–dispersed CNTs (0.045 *vs.* 0.016 Ω cm at 25 °C), with <10% variation between 25 and 50 °C. This unique balance between enhanced aqueous dispersibility and preserved charge transport underscores $ClO_2^{\bullet}$ oxidation as a green and effective strategy for producing water-processable CNTs, showing promise for applications in pharmaceutical drugs, printable electronics, functional composites, energy storage, and sensing.

Received 25th December 2025,
Accepted 9th February 2026

DOI: 10.1039/d5nr05444c

rsc.li/nanoscale

Introduction

Carbon nanotubes (CNTs) have attracted tremendous attention since their discovery by Iijima in 1991 [1] owing to their unique one-dimensional nanostructures and outstanding physicochemical properties. Single-walled carbon nanotubes (SWCNTs) have nanometer-scale diameters and micrometer-to-millimeter-scale lengths,[2] resulting in extremely high aspect ratios. These structural characteristics endow CNTs with exceptional electrical conductivity,[3] mechanical strength,[4] thermal conductivity,[5] and optical responses.[6] As a result, CNTs have been extensively investigated as key materials in a wide variety of fields ranging from nanoelectronics and transparent conductive films[7] to energy conversion and storage devices,[8–10] catalyst supports,[11] biosensors,[12] and drug delivery platforms.[13] Their versatile electronic behaviour, whether metallic or semiconducting, further expands their technological potential, particularly for next-generation field-effect transistors, photovoltaics, and optoelectronic devices.[14]

Despite these attractive features, the most critical challenges hindering the practical use of CNTs are their poor solubility and dispersibility in aqueous media.[15] CNTs are intrinsically hydrophobic and tend to aggregate into bundles *via* strong van der Waals interactions.[16] Such aggregation not only decreases their processability but also prevents the manifestation of their intrinsic electronic, optical, and mechanical properties, ultimately limiting their usefulness in real-world applications. Therefore, the development of strategies to achieve stable, uniform, and surfactant-free dispersion of CNTs in polar solvents, particularly water, remains a central issue in CNT research.[17,18]

Numerous approaches have been proposed to address this issue. Physical dispersion *via* ultrasonication in the presence of surfactants is the most commonly used method.[19] Surfactants such as sodium dodecyl sulfate or bile salts stabilize CNTs by forming micelle-like structures around them. However, surfactant molecules that persist on the CNT surfaces can interfere with the interfacial properties, degrade the electrical conductivity, and complicate subsequent functionali-

[a]*Institute for Open and Transdisciplinary Research Initiatives (OTRI), The University of Osaka, 1-6 Yamada-oka, Suita, Osaka, 565-0871, Japan.*
E-mail: ohkubo@irdd.osaka-u.ac.jp
[b]*Frontier Research Institute for Interdisciplinary Sciences (FRIS), Tohoku University, 6-3 Aramaki-aza-aoba, Aoba-ku, Sendai, Miyagi, 980-8578, Japan*
[c]*Department of Chemistry, Graduate School of Science, Tohoku University, 6-3 Aramaki-aza-aoba, Aoba-ku, Sendai, Miyagi, 980-8578, Japan*
[d]*Idea International Co., Ltd., 1-2-11 Kitayama Aoba-ku, Sendai, Miyagi 981-0931, Japan*
[e]*Organization for Carbon Neutrality Collaboration (OCNC), The University of Osaka, 1-6 Yamada-oka, Suita, Osaka, 565-0871, Japan*

zation, making this method less desirable for applications requiring pristine electronic characteristics. Polymer-assisted dispersion offers another route in which polymers noncovalently interact with CNTs to prevent aggregation.[20] Although this method provides relatively good stability, strong polymer–CNT interactions can alter the surface chemistry and diminish the intrinsic properties.[21]

Therefore, chemical functionalization has been widely explored as an alternative approach.[21,22] In particular, oxidative treatments introduce polar oxygen-containing groups, such as hydroxy, carbonyl, and carboxy moieties, onto CNT surfaces, thereby improving their dispersibility in polar solvents.[23,24] Nitric and sulfuric acid treatments are the most established methods and are often performed under reflux conditions.[25] While effective in enhancing water dispersibility, these methods typically involve harsh reaction conditions, which can cause significant structural degradation, shortening of CNTs, or even destruction of their π-conjugated framework.[24] Such damage reduces the electrical and mechanical performance of CNTs and compromises their environmental safety and scalability. These drawbacks highlight the urgent need for milder, more selective, environmentally benign oxidation strategies.[26,27]

In this regard, chlorine dioxide ($ClO_2^{\bullet}$) represents an attractive alternative. $ClO_2^{\bullet}$ is a highly selective and mild oxidant with a high redox potential, enabling efficient oxidation under ambient conditions.[28] Its industrial relevance is well established: for decades, $ClO_2^{\bullet}$ has been widely used in water purification, disinfection, and pulp bleaching owing to its powerful oxidizing ability and relatively low environmental impact. Importantly, $ClO_2^{\bullet}$ can be readily generated in aqueous solution by acidifying sodium chlorite ($NaClO_2$) with hydrochloric acid,[28–32] offering a simple, cost-effective, and scalable means of preparation.

In organic synthesis, $ClO_2^{\bullet}$ and related chlorite reagents have been used to oxidize sulfides. For example, sodium chlorite combined with hydrochloric acid facilitates sulfide oxidation into sulfones,[29] whereas tetrabutylammonium chlorite has been employed as a tunable oxidant that selectively produces sulfoxides under controlled conditions.[30] Moreover, under photoirradiation, $ClO_2^{\bullet}$ can undergo homolysis to generate chlorine radicals and singlet oxygen, which are harnessed in chlorine-radical-mediated C–H oxygenation reactions.[31] These studies highlight the versatility of chlorine-based oxidants in selective organic transformations. Nevertheless, their application to CNT surface modification remains underexplored, providing a significant opportunity to develop green and efficient oxidation strategies.

Herein, we demonstrate that $ClO_2^{\bullet}$ enables surfactant-free dispersion of SWCNTs in water under ambient conditions while preserving their tubular morphology and intrinsic conductivity. The treatments at room temperature selectively introduced hydroxy, carbonyl, and carboxy functionalities, leading to stable aqueous dispersions with a ζ potential of −41.6 mV, indicative of substantial electrostatic stabilization. Structural analyses using X-ray photoelectron spectroscopy (XPS), Raman spectroscopy, and transmission electron microscopy (TEM) confirmed controlled surface oxidation (~12% oxygen incorporation) without severe lattice degradation. Importantly, films prepared from these dispersions exhibited only a modest threefold increase in resistivity (0.045 Ω cm *vs.* 0.016 Ω cm for surfactant-dispersed CNTs), retaining high electronic performance. By contrast, heating the $ClO_2^{\bullet}$ solution to 80 °C led to poor dispersibility, formation of non-tubular aggregates, and loss of CNT structural integrity, highlighting the selectivity of the room-temperature process. Therefore, $ClO_2^{\bullet}$-based oxidation is a green, mild, and effective strategy for preparing water-dispersible CNTs. Balancing hydrophilization with conductivity preservation avoids the drawbacks of conventional strong-acid oxidation and surfactant stabilization. We anticipate that this approach will broaden the utility of CNTs in environmentally sensitive applications, including electronics, energy devices, catalysis, and biomedical technologies, while contributing to the sustainable development of carbon nanomaterials.

Experimental

Reagents

Sodium chlorite ($NaClO_2$, ≥80%, Sigma-Aldrich) and hydrochloric acid (HCl, 35 wt%, Kishida Chemical Co.) were purchased and used as received without further purification. Single-walled carbon nanotubes (SWCNTs, eDIPS EC-2.0P, Meijo Nano Carbon Co., Ltd) were employed as the primary material in this study. Sodium cholate (TCI) was used for preparing control dispersions. All other chemicals and solvents were of analytical grade and used as received. Ultrapure water (Milli-Q system, Merck Millipore) was used in all experiments.

Instrumentation

Transmission electron microscopy (TEM) images were obtained using a JEOL JEM-2100 microscope operated at 200 kV. Raman spectra were recorded with a Raman spectrometer (Raman Force, Nanophoton Co. Ltd, Osaka, Japan) equipped with a 532 nm excitation laser. Dynamic light scattering (DLS) and ζ-potential measurements were performed using an ELSZ-2000S particle size and molecular weight measurement system (Otsuka Electronics Co., Ltd). X-ray photoelectron spectroscopy (XPS) was carried out on a Shimadzu Kratos ULTRA2 spectrometer using monochromatic Al Kα radiation (1486.6 eV). Electrical resistivity of CNT films was measured by the standard four-probe method using a nano-voltmeter (Keithley 2182A) coupled with a DC/AC current source (Keithley 6221). For removal of thermal offsets and electrical noise, we employed the delta mode (averaging three measurements with alternating polarity).

Oxidation and surfactant-free dispersion of SWCNTs

Chlorine dioxide ($ClO_2^{\bullet}$) solution was prepared by adding 300 μL of 35% aqueous hydrochloric acid to an aqueous solution of sodium chlorite (300 mg in 30 mL of water) in a glass

vial. Single-walled carbon nanotubes (SWCNTs, eDIPS EC-2.0P, diameter 2.0–3.0 nm, 10.5 mg) were then introduced into the solution. The mixture was sonicated for 1 h at 40 kHz and subsequently stirred at 25 °C for 6 days using a magnetic stirrer. After the reaction, the suspension was filtered through a hydrophilic PTFE membrane (pore size 0.2 μm), and the collected solid was thoroughly washed with ultrapure water.

The recovered SWCNTs were transferred to a fresh glass vessel containing a newly prepared chlorine dioxide solution, followed by sonication for 1 h at 40 kHz and stirring at 25 °C for an additional 7 days. The dispersion was filtered again through a hydrophilic PTFE membrane (0.2 μm), and the resulting solid was washed with water and dried under vacuum. The final product, oxidized SWCNTs, was obtained as a black powder (12.1 mg).

Results and discussion

Chlorine dioxide ($ClO_2^{\bullet}$) was generated by reacting sodium chlorite ($NaClO_2$) with hydrochloric acid (eqn (1)).[33]

$$5NaClO_2 + 4HCl \rightarrow 4\ ClO_2^{\bullet} + 2\ H_2O + 5\ NaCl \qquad (1)$$

This highly reactive yellow gas exhibits a pronounced absorption maximum at 358 nm.[31,32] After acidifying an aqueous sodium chlorite solution with hydrochloric acid, the solution turned yellow, confirming the formation of $ClO_2^{\bullet}$. Introduction of carbon nanotubes (CNTs) into the resulting $ClO_2^{\bullet}$ solution (0.10 M) followed by stirring at room temperature led to the gradual oxidative dispersion of CNT aggregates (Scheme 1). This process is ascribed to surface functionalization by $ClO_2^{\bullet}$, which introduces hydrophilic oxygenated groups, such as hydroxy and carboxy functionalities, thereby enhancing their dispersibility in water. After reacting for 2 h, large bundles of CNTs were observed. However, from 17 h onward, these aggregates gradually became finer, and by 22 h the suspension was more homogeneous, although the yellow coloration of $ClO_2^{\bullet}$ was still visible (Fig. 1). Prolonged stirring for 14 days ultimately afforded a stable black dispersion of oxidized CNTs.

The control experiments further substantiated the central role of $ClO_2^{\bullet}$. At 80 °C, CNT aggregates initially dispersed within 2 h, and extensive dispersion was observed after 17 h. Prolonged heating, however, led to the disappearance of the characteristic black coloration by 22 h, and filtration and

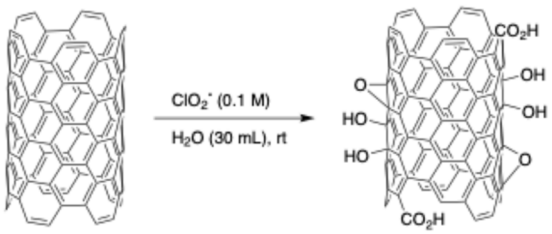

Scheme 1 CNT oxidation in an aqueous $ClO_2^{\bullet}$ solution.

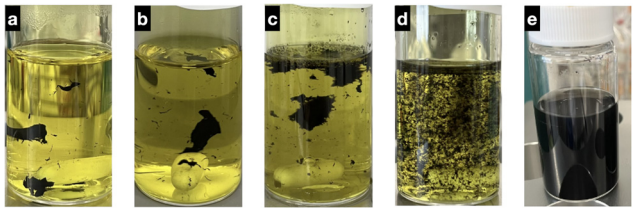

Fig. 1 Photographic images showing the time-dependent dispersion of CNTs (10.5 mg) in an aqueous $ClO_2^{\bullet}$ solution (0.10 M, 30 mL) stirred by a magnetic stirrer at room temperature for (a) 0 h; (b) 2 h; (c) 17 h; (d) 22 h; (e) 14 days.

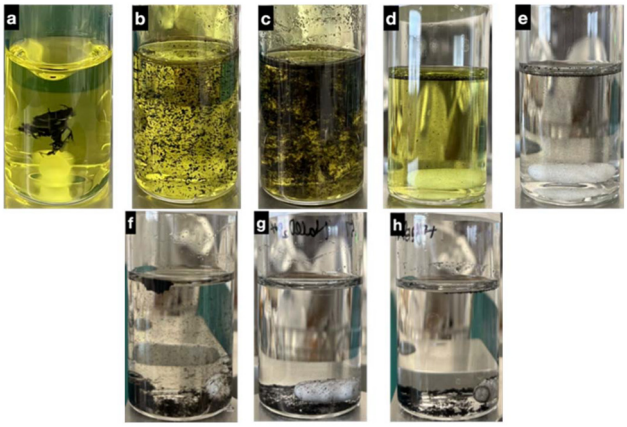

Fig. 2 Photographic images of control experiments for CNT oxidation and dispersion. Top: Time-dependent behavior at 80 °C. (a) 0 h; (b) 2 h; (c) 17 h; (d) 22 h; (e) sample after 22 h followed by quenching of $ClO_2^{\bullet}$ with 365 nm irradiation. Bottom: Reactions conducted under alternative conditions. (f) CNT oxidation under 365 nm irradiation in the presence of $ClO_2^{\bullet}$; (g) $NaClO_2$ only, heated at 80 °C; (h) HCl only, heated at 80 °C.

washing afforded only a gray solid, indicating progressive degradation rather than stable dispersion (Fig. 2). The reactions were performed under UV light. When the reaction was carried out under UV irradiation (365 nm), $ClO_2^{\bullet}$ rapidly decomposed into chlorine radicals and singlet oxygen, reactive species that are sufficiently potent to oxidize methane.[31] Under these conditions, $ClO_2^{\bullet}$ was consumed before engaging with the CNT surface, and dispersion was not achieved. Similarly, heating the sodium chlorite solution in the absence of hydrochloric acid produced no dispersion, indicating that chlorite ions alone were incapable of initiating oxidation. In addition, the CNTs stirred in hydrochloric acid alone showed no detectable changes, even when heated. Collectively, these findings clearly demonstrate that $ClO_2^{\bullet}$ is the key oxidant responsible for selective surface functionalization and aqueous dispersion of CNTs under mild, additive-free conditions. Dynamic light scattering (DLS) analysis of the oxidized dispersion, after removal of residual large particulates by centrifugation and subsequent dilution of the supernatant, revealed two distinct size populations at 1.9 ± 0.4 nm and 279 ± 105 nm (Fig. 3). The larger fraction corresponds to dispersed

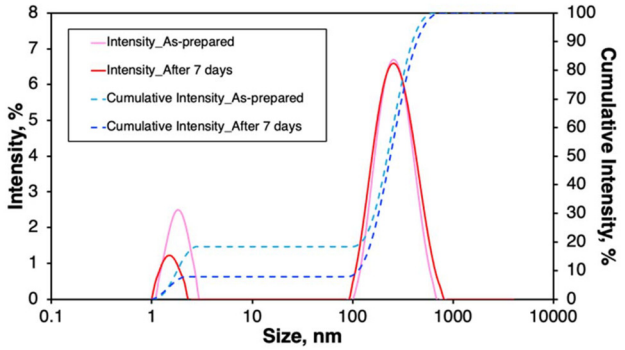

Fig. 3 DLS size distributions of oxidized CNT dispersions.

CNTs, whereas the smaller fraction is most reasonably attributed to oxidatively cleaved CNT fragments with limited length rather than intact long tubes, because DLS reports an apparent hydrodynamic radius based on a spherical model and does not yield such a small value for extended nanotubes. Notably, DLS analysis performed after 7 days showed essentially unchanged size distributions, with two populations centered at 1.5 ± 0.3 nm and 287 ± 125 nm, indicating that no significant aggregation or growth of dispersed particles occurred over this period. The dispersion remained stable without visible precipitation for at least one week. A ζ potential of −41.6 ± 1.9 mV confirmed the introduction of negatively charged oxygenated groups on the CNT surface, providing sufficient electrostatic repulsion to ensure colloidal stability. This stabilization mechanism is conceptually analogous to that of surfactant-assisted dispersions but is achieved without residual surfactants. The pronounced negative ζ potential is consistent with Derjaguin–Landau–Verwey–Overbeek-type electrostatic stabilization arising from deprotonated oxygenated groups,[24,34] as also supported by XPS signatures (C–O, C═O, and COO functionalities). Together, these results indicate that the $ClO_2^{\bullet}$ treatment yields aqueous dispersions stabilized by electrostatic repulsion; a fraction of the nanotubes exist as oxidatively shortened fragments, while larger clusters remain detectable within the broader size fraction. TEM images of the room-temperature-treated dispersion revealed micrometer-scale fibrous features attributable to the CNTs (Fig. 4a).

At higher magnifications, individual nanotubes were clearly resolved, showing uniform diameters and continuous tubular frameworks without any signs of collapse (Fig. 4b). These observations indicate that the oxidation proceeds in a surface-limited manner, introducing functional groups while preserving the underlying sp^2 network.[22,24] This structural integrity is consistent with the Raman spectra, which retained a pronounced G band despite the emergence of the D band.[15,24]

By contrast, the TEM images of the solid obtained at 80 °C did not display a tubular morphology but rather sheet-like and amorphous aggregates (Fig. 4c). This morphology reflects over-oxidation, in which C–C bond cleavage leads to structural degradation rather than stable functionalization.[25] Taken together, the TEM results highlight the divergent outcomes of

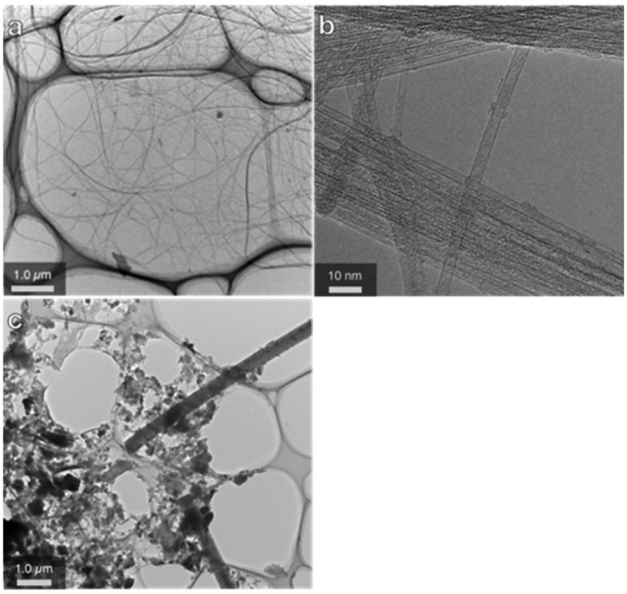

Fig. 4 TEM images of Ox-CNTs: (a) wide-field image at the micrometer scale showing fibrous features consistent with carbon nanotubes; (b) higher-magnification image indicating that the tubular framework was preserved; (c) image of the white precipitate obtained after heating at 80 °C, showing sheet-like aggregates instead of tubular structures.

$ClO_2^{\bullet}$ oxidation: at room temperature, selective functionalization preserves the nanotube framework and enables aqueous dispersion, whereas under heating, uncontrolled over-oxidation causes structural degradation and complete loss of the tubular morphology.

Raman spectroscopy was used to investigate the structural integrity of the oxidized nanotubes (Fig. 5). For comparison, pristine CNTs were dispersed in water with 1 wt% sodium cholate, filtered through a membrane, washed, and measured as thin films. In the Raman spectra of the CNTs, the G band at

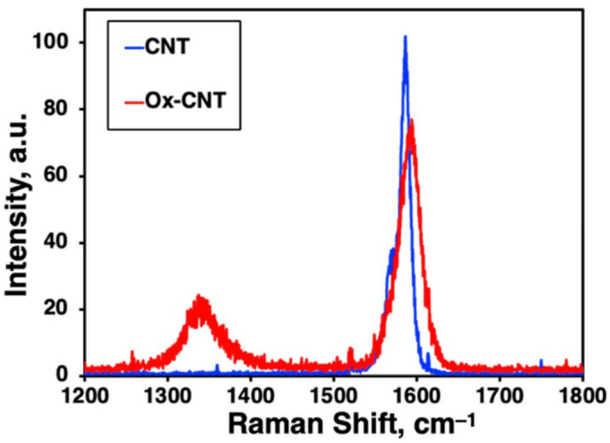

Fig. 5 Raman spectra of thin films of pristine and oxidized CNTs, prepared by filtering aqueous dispersions. Pristine CNTs were dispersed using 1 wt% sodium cholate.

~1590 cm^{-1} corresponds to the in-plane vibration of sp^2-hybridized carbon atoms in the hexagonal lattice, whereas the D band at ~1350 cm^{-1} originates from disordered carbon atoms with dangling bonds.[35,36] The intensity ratio of these bands (G/D) is widely used to evaluate the structural disorder induced by oxidation.[15,24,37]

The pristine CNTs exhibited a sharp G band with no detectable D band, which is consistent with intact sp^2 frameworks. By contrast, the spectrum of the oxidized CNTs showed a broadened G band and a pronounced D band at 1350 cm^{-1}. The G/D ratio of 3.5 indicates that oxidative defects were introduced, whereas the sp^2 carbon network was largely retained. The broadening of the G band reflects local lattice distortions induced by the oxygenated groups, and the emergence of the D band highlights the creation of defect sites that act as scattering centers.[24,35] These features are in line with TEM observations of preserved tubular morphology and with XPS evidence of oxygen incorporation, collectively pointing to surface-limited functionalization by $ClO_2^{\bullet}$. This process introduces sufficient hydrophilic groups for aqueous dispersion while avoiding extensive lattice destruction, thereby rationalizing the modest increase in resistivity observed for the oxidized CNT films. XPS analysis revealed atomic contents of 99.6% C, 0.3% O, and 0.1% Cl for the pristine CNTs, whereas the oxidized CNTs contained 89.0% C, 10.6% O, and 0.4% Cl.

These values correspond to ~12% oxygen incorporation relative to carbon, with negligible chlorine retention. The high-resolution C 1s spectra provide more detailed insights into the chemical states (Fig. 6). The spectrum of the pristine sample was dominated by the sp^2 C═C peak at ~284.8 eV. Minor oxygen contributions were unresolved in the fitting because the elemental analysis indicated a negligible oxygen content (0.3%) at 285–290 eV. The weak features observed above 290 eV are attributed to π–π* peak associated with sp^2-hybridized carbon.

By contrast, the oxidized CNTs exhibited additional components assigned to C–O (5.1% at ~286.3 eV), C═O (3.1% at ~287.9 eV), and O–C═O (2.6% at ~289.2 eV) groups.[22,24] These oxygenated functionalities are consistent with the introduction of hydroxy, carbonyl, and carboxy groups onto the CNT surface.

The relative distribution of these oxygenated species indicated that the majority of the oxygen was incorporated as C–O functionalities, with lower yet still significant fractions of C═O and O–C═O. The oxygenated shoulder peaks accompanying the dominant sp^2 C═C peak further support the occurrence of surface-limited functionalization rather than bulk lattice disruption,[15,24] which agrees with the TEM images and Raman spectra. Such oxygenated groups also provide a structural basis for the strongly negative ζ potential (−41.6 mV), which accounts for the electrostatic stabilization of the aqueous dispersion.[15]

Chlorine was detected only at trace levels (0.4%), indicating that any residual chlorine species were effectively removed during washing. Taken together, the XPS results demonstrate that $ClO_2^{\bullet}$ selectively introduces oxygen-containing groups at the CNT surface, enabling stable dispersion without compromising the underlying sp^2 framework.

Films prepared by filtering the dispersions exhibited a volume resistivity of 0.016 Ω cm for sodium cholate–dispersed CNTs and 0.045 Ω cm for oxidized CNTs at 25 °C, corresponding to only a threefold increase (Fig. 7). Notably, from 25 to 50 °C, the resistivity of the oxidized CNTs increased by less than 10%, indicating that the electronic conductivity was mostly preserved, despite the introduction of surface oxygen functionalities. The minimal temperature dependence indicates that the charge transport in the oxidized CNT films is dominated by a percolated sp^2 network rather than by thermally activated hopping. Although the absolute resistivity of the oxidized films was higher than that of the sodium cholate–dispersed CNTs, the values remained within the typical range for conductive CNT networks.[7,9] This modest trade-off highlights that $ClO_2^{\bullet}$ oxidation substantially improves dispersibility while preserving electronic pathways, offering a favorable balance for applications that demand both aqueous processability and reliable charge transport under variable thermal conditions, such as printable electronics, composite conductors, and energy storage devices.[13,27]

This behavior can be rationalized by the surface-selective nature of the $ClO_2^{\bullet}$ oxidation, which predominantly introduces oxygenated functionalities at defect sites and exposed structurally accessible regions of the carbon nanotubes without extensive disruption of the underlying sp^2 lattice. These accessible regions correspond to tube ends, intrinsic defect sites, and

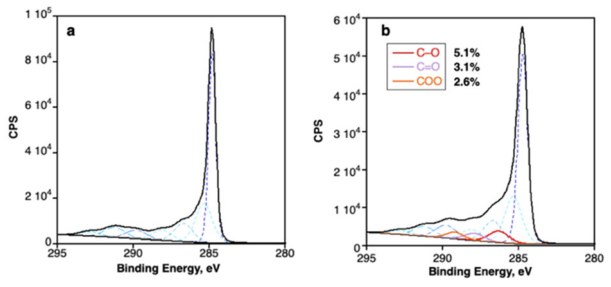

Fig. 6 XPS spectra of (a) pristine CNTs and (b) oxidized CNTs with Gauss-Lorentz fitting curves.

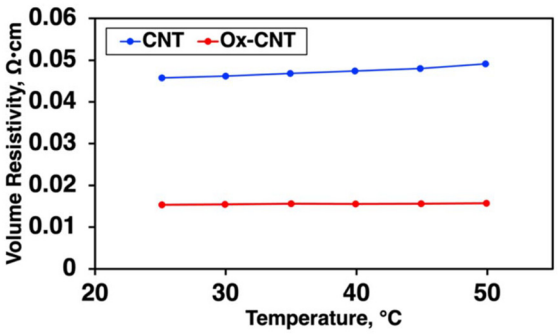

Fig. 7 Volume resistivity of CNT films prepared by filtration: pristine CNTs dispersed with sodium cholate (blue) and oxidized CNTs (red).

externally exposed sidewall surfaces of individual tubes or bundle surfaces. In contrast to stronger oxidative treatments that generate a high density of basal-plane defects, the present oxidation proceeds in a spatially confined manner, allowing the graphitic core and percolated conductive pathways to remain largely intact. As a result, even with an oxygen content of approximately 12%, the electrical conductivity is retained because charge transport is governed by continuous sp^2 domains rather than by localized hopping through heavily oxidized regions. In this context, $ClO_2^{\bullet}$ can be regarded as a relatively mild and selective oxidant under the present conditions, providing a mechanistic basis for the observed balance between enhanced dispersibility and preserved electrical performance.

Conclusions

In this work, we developed and systematically evaluated a green and versatile approach for dispersing SWCNTs in water through chlorine dioxide ($ClO_2^{\bullet}$)-mediated oxidation under ambient conditions. The $ClO_2^{\bullet}$ oxidation reported herein enables mild, selective, and scalable oxidation that enhances aqueous dispersibility while mostly maintaining the intrinsic electronic functionality of the CNT framework. This methodology addresses a long-standing challenge in CNT processing by combining dispersion stability with minimal compromise in conductivity. The unique property profile achieved here expands the potential of CNTs for environmentally sensitive applications in which both dispersibility and electronic performance are critical, including printable electronics, functional polymer composites, electrochemical energy storage, and sensing platforms.

Author contributions

Yuki Itabashi: Conceptualization, investigation, data curation, visualization, writing – original draft, writing – review & editing. Ai Sunami: Investigation, formal analysis, data curation. Kaoru Maeno: Investigation, formal analysis. Hiroshi Ueno: Investigation, formal analysis. Takashi Itoh: Investigation, formal analysis. Hiroshi Fukumura: Investigation, formal analysis. Kei Ohkubo: Conceptualization, supervision, project administration, writing – review & editing, funding acquisition.

Conflicts of interest

The authors declare no conflict of interest.

Data availability

The data that support the findings of this study are available from the corresponding author (K. O.) upon reasonable request.

Acknowledgements

The authors are grateful to Mr Yosuke Murakami (The Institute of Scientific and Industrial Research, The University of Osaka) for his assistance with TEM measurements. This work was carried out using research equipment shared under the MEXT Project for Promoting Public Utilization of Advanced Research Infrastructure (Program for Supporting Construction of Core Facilities), Grant Number JPMXS0441200023. We also thank Dr Yasuhiko Kasama (Idea International Co., Ltd) for providing access to the equipment used for volume resistivity measurements. Financial support from JSPS KAKENHI (Grant Numbers JP23K13709 to Y. I. and JP24K21770 to K. O.) is gratefully acknowledged.

References

1 S. Iijima, *Nature*, 1991, **354**, 56–58.
2 S. Iijima and T. Ichihashi, *Nature*, 1993, **363**, 603–605.
3 S. Frank, P. Poncharal, Z. L. Wang and W. A. de Heer, *Science*, 1998, **280**, 1744–1746.
4 M. M. J. Treacy, T. W. Ebbesen and J. M. Gibson, *Nature*, 1996, **381**, 678–680.
5 P. Kim, L. Shi, A. Majumdar and P. L. McEuen, *Phys. Rev. Lett.*, 2001, **87**, 215502.
6 S. M. Bachilo, M. S. Strano, C. Kittrell, R. H. Hauge, R. E. Smalley and R. B. Weisman, *Science*, 2002, **298**, 2361–2366.
7 Z. Wu, Z. Chen, X. Du, J. M. Logan, J. Sippel, M. Nikolou, K. Kamaras, J. R. Reynolds, D. B. Tanner, A. F. Hebard and A. G. Rinzler, *Science*, 2004, **305**, 1273–1276.
8 T. Umeyama and H. Imahori, *Energy Environ. Sci.*, 2008, **1**, 120–133.
9 M. Kaempgen, G. S. Duesberg and S. Roth, *Appl. Surf. Sci.*, 2005, **252**, 425–429.
10 S. Aoi, K. Mase, K. Ohkubo, T. Suenobu and S. Fukuzumi, *ACS Energy Lett.*, 2017, **2**, 4077–4081.
11 P. Serp, M. Corrias and P. Kalck, *Appl. Catal., A*, 2003, **253**, 337–358.
12 J. Wang, *Electroanalysis*, 2005, **17**, 7–14.
13 K. Kostarelos, A. Bianco and M. Prato, *Nat. Nanotechnol.*, 2009, **4**, 627–633.
14 A. Javey, J. Guo, Q. Wang, M. Lundstrom and H. Dai, *Nature*, 2003, **424**, 654–657.
15 S. Niyogi, M. A. Hamon, H. Hu, B. Zhao, P. Bhowmik, R. Sen, M. E. Itkis and R. C. Haddon, *Acc. Chem. Res.*, 2002, **35**, 1105–1113.
16 J. Chen, M. A. Hamon, H. Hu, Y. Chen, A. M. Rao, P. C. Eklund and R. C. Haddon, *Science*, 1998, **282**, 95–98.
17 V. C. Moore, M. S. Strano, E. H. Haroz, R. H. Hauge, R. E. Smalley, J. Schmidt and Y. Talmon, *Nano Lett.*, 2003, **3**, 1379–1382.
18 B. I. Kharisov, O. V. Kharissova, H. L. Gutierrez and U. O. Méndez, *Ind. Eng. Chem. Res.*, 2009, **48**, 572–590.

19 M. J. O'Connell, S. M. Bachilo, C. B. Huffman, V. C. Moore, M. S. Strano, E. H. Haroz, K. L. Rialon, P. J. Boul, W. H. Noon, C. Kittrell, J. Ma, R. H. Hauge, R. B. Weisman and R. E. Smalley, *Science*, 2002, **297**, 593–596.
20 M. Zheng, A. Jagota, E. D. Semke, B. A. Diner, R. S. McLean, S. R. Lustig, R. E. Richardson and N. G. Tassi, *Nat. Mater.*, 2003, **2**, 338–342.
21 D. Tasis, N. Tagmatarchis, A. Bianco and M. Prato, *Chem. Rev.*, 2006, **106**, 1105–1136.
22 A. Hirsch, *Angew. Chem., Int. Ed.*, 2002, **41**, 1853–1859.
23 A. Hirsch and O. Vostrowsky, *Top. Curr. Chem.*, 2005, **245**, 193–237.
24 V. Datsyuk, M. Kalyva, K. Papagelis, J. Parthenios, D. Tasis, A. Siokou, I. Kallitsis and C. Galiotis, *Carbon*, 2008, **46**, 833–840.
25 A. Kuznetsova, D. B. Mawhinney, V. Naumenko, J. T. Yates, J. Liu and R. E. Smalley, *Chem. Phys. Lett.*, 2000, **321**, 292–296.
26 T. Lien, N. Madoka, K. Ishihara, K. Oyama, S. Fujii and S. Yusa, *Polym. J.*, 2021, **53**, 1001–1009.
27 B. F. Machado and P. Serp, *Catal. Sci. Technol.*, 2012, **2**, 54–75.
28 Y. Itabashi, H. Asahara and K. Ohkubo, *Chem. Commun.*, 2023, **59**, 7506–7509.
29 Y. Itabashi, S. Ogata, T. Inoue, H. Asahara and K. Ohkubo, *Molecules*, 2025, **30**, 1912.
30 Y. Itabashi, S. Ogata, Y. Shimada, M. Kondo, N. Nishiwaki, T. Inoue, H. Asahara and K. Ohkubo, *Chem. – Eur. J.*, 2025, **31**, e202404279.
31 K. Ohkubo and K. Hirose, *Angew. Chem., Int. Ed.*, 2018, **57**, 2126–2129.
32 K. Ohkubo, K. Hirose, T. Shibata, K. Takamori and S. Fukuzumi, *J. Phys. Org. Chem.*, 2017, **30**, e3619.
33 B. R. Deshwal, H.-D. Jo and H.-K. Lee, *Can. J. Chem. Eng.*, 2004, **82**, 619–624.
34 R. J. Hunter, *Zeta Potential in Colloid Science*, Academic Press, London, 1981.
35 A. C. Ferrari and J. Robertson, *Phys. Rev. B: Condens. Matter Mater. Phys.*, 2000, **61**, 14095–14107.
36 A. Jorio, M. A. Pimenta, A. G. Souza Filho, R. Saito, G. Dresselhaus and M. S. Dresselhaus, *New J. Phys.*, 2003, **5**, 139.
37 H. Hu, B. Zhao, M. A. Hamon, K. Kamaras, M. E. Itkis and R. C. Haddon, *J. Am. Chem. Soc.*, 2003, **125**, 14893–14900.